Investigation of anisotropic epoxy-amine thermosets synthesised in a magnetic field

Laurence Pottié[ab]; France Costa-Torro[ab]; Martine Tessier[ab]; Patrick Davidson[cd]; Alain Fradet[ab]

[a] Université Pierre et Marie Curie-Paris 6, Laboratoire de Synthèse Macromoléculaire, 75252 Paris Cedex 05, France [b] CNRS, U.M.R., Paris, France [c] Université Paris-Sud, Laboratoire de Physique des Solides, 91405 Orsay Cedex, France [d] CNRS, U.M.R., Orsay, France

PLEASE SCROLL DOWN FOR ARTICLE

Taylor & Francis
Taylor & Francis Group

Investigation of anisotropic epoxy–amine thermosets synthesised in a magnetic field

Laurence Pottié[ab], France Costa-Torro[ab], Martine Tessier[ab], Patrick Davidson[cd] and Alain Fradet[ab]*

[a]*Université Pierre et Marie Curie-Paris 6, Laboratoire de Synthèse Macromoléculaire, 4 Place Jussieu, 75252 Paris Cedex 05, France;* [b]*CNRS, U.M.R. n° 7610, Paris, France;* [c]*Université Paris-Sud, Laboratoire de Physique des Solides, Bâtiment 510, 91405 Orsay Cedex, France;* [d]*CNRS, U.M.R. n° 8502, Orsay, France*

Bis{4-[2-(2,3-epoxypropyl)ethoxy]benzoate}-1,4-phenylene and bis[4-(2,3-epoxypropoxy)benzoate]-methyl-1,4-phenylene liquid crystalline diepoxy monomers were crosslinked with various diamines in a magnetic field. X-ray scattering was used for mesophase identification and to determine the nematic order parameter of the resulting thermosets, which were cured under various temperature and magnetic field strength conditions. All thermosets exhibited nematic or smectic A (SmA) mesophases. The thermosets obtained from aliphatic diamines exhibited a very low degree of orientation. This phenomenon was assigned to their high reactivity, inducing a very fast crosslinking reaction that prevents the alignment of the mesogens. On the other hand, very high degrees of orientation along the magnetic field axis were observed for the SmA thermosets. In this case, the smectic period was smaller than the length of the epoxy monomer unit, which might be due to a staggered packing of the mesogenic cores. Negative longitudinal thermal expansion coefficients were measured below and above the glass transition temperature for the materials cured in a magnetic field.

Keywords: liquid crystal polymers; thermosets; magnetic field curing

1. Introduction

The physical properties of polymers strongly depend on their orientational order (*1, 2*). One of the methods by which ordered polymeric structures can be obtained is through self-organising systems such as liquid crystals (LCs). It is well known that superior mechanical properties can be obtained by achieving a high degree of molecular alignment in liquid-crystal-line polymers (*3*). This alignment is usually induced by extensional flow during melt extrusion with the resulting orientation being stronger near the surface than in the centre of the sample (*4*). Specific surfaces can also be used to orient lyotropic polymers in order to obtain thin ordered films. On the other hand, magnetic (*5–9*) and electric (*10, 11*) fields have proven to be very suitable to obtain ordered structures, homogeneously throughout the bulk. In this context, the synthesis of "liquid-crystalline" thermosets (LCTs) appears of particular interest. LCTs can be defined as crosslinked materials exhibiting a LC-like organisation. They are most often obtained by curing a LC monomer or a LC oligomer in the anisotropic state (*12*). When the curing reaction is carried out in a magnetic field, the LC organisation is preserved in the final network, resulting in polymers with highly ordered internal structure (*13, 14*). LC monomers containing various crosslinkable groups, such as acrylate, methacrylate, epoxy, vinyl ether, maleimide, nadimide, diene an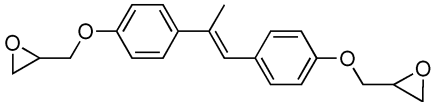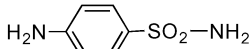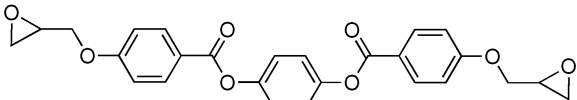d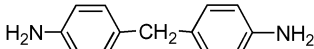 acetylene, have been used for the synthesis of anisotropic networks (*15*). Only a few systems have been oriented and crosslinked in a magnetic field, mainly LC epoxy monomers with diamines (Table 1). Similar to aligned LC polymers, highly oriented networks exhibit properties that are strongly anisotropic. For example, the coefficient of linear thermal expansion (CTE) of such materials will be considerably lower in the field direction ($CTE_{//}$) than in the perpendicular direction ($CTE_{\perp}$) (*16*). If the orientation is strong enough, a negative $CTE_{//}$ can even be observed, meaning that the material shrinks with increasing temperature. In particular, Jahromi *et al.* crosslinked PEEB–benzidine epoxy–amine systems (Table 1) in a magnetic field and reported a negative $CTE_{//}$ for the final materials (*17*).
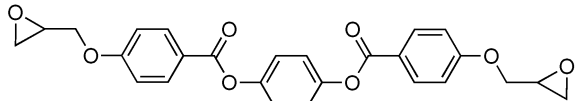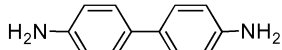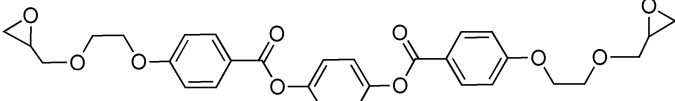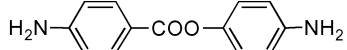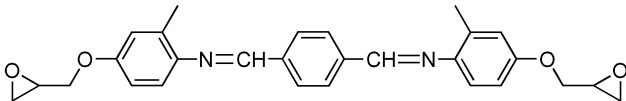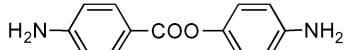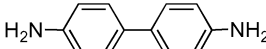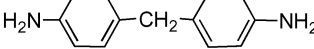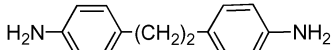
In order to study materials exhibiting negative $CTE_{//}$, we first investigated the PEEB–benzidine system by varying curing conditions (time, temperature, magnetic field strength), by exploring reaction kinetics and by determining the structure of final thermosets by X-ray scattering. We then compared it to the MPEPB–benzidine system (*28*) (Table 2).

Both PEEB and MPEPB have a broad nematic range and thus are convenient for the synthesis of ordered networks. They possess a triphenyl ester mesogenic core, but MPEPB has no spacer between its central core and the oxirane ring. This makes it less flexible than PEEB and we can therefore expect to obtain materials with higher modulus. On the other hand, MPEPB has a methyl group on the

---

*Corresponding author. Email: alain.fradet@upmc.fr

Table 1. Diepoxy/diamine systems cured under a magnetic field, as reported in the literature.
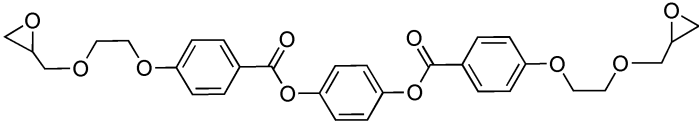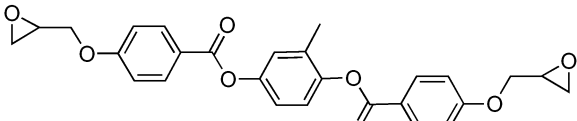
Diepoxy	Diamine	Ref.
EPAMS	SAA	(*13, 16, 18–21*)
	MDA	(*22, 23*)
PEPB	benzidine	(*24*)
		(*25*)
R = CH₃, Cl		(*25*)
PEEB	benzidine	(*17, 26*)
	MDA	(*17*)
DGETAM	DDE	(*27*)

central ring of its mesogenic core. This could have an adverse effect on the order of the material by disturbing the lateral packing of the mesogens. Nevertheless, Mormann *et al.* observed the formation of an anisotropic phase upon reacting this monomer with aromatic diamines (*28, 29*).

In a second step we broadened our study by reacting both PEEB and MPEPB with various

Table 2. Structures, names, abbreviations and transition temperatures of the diepoxy compounds used in this study.

Structure, chemical name and abbreviation	$T /°C^a$
1,4-phenylenebis(4-(2-(2,3-epoxypropoxy)ethoxy)benzoate) (PEEB)	Cr 124.7 N 184.5 I
methyl-1,4-phenylenebis(4-(2,3-epoxypropoxy)benzoate) (MPEPB)	Cr 135.5 N 229.3 I

[a] Cr=crystal; N=nematic; I=isotropic.

diamines, in order to understand the role of cross-linker structure on thermoset properties. For this purpose, three types of diamines were used: linear aliphatic diamines, symmetric aromatic diamines and asymmetric diamines where the two amine functions have very different reactivities (Table 3). The nature of mesophases and the degree of orientation of these thermosets were investigated by X-ray scattering. Finally, CTE$_{//}$ measurements were carried out on some of these samples in order to gain a better insight into the CTE–orientation relationships for this type of material.

2. Experimental

Materials

All chemicals were obtained from Aldrich Chemical Co and used as received, except pyridine and thionyl chloride, which were distilled before use. The molecular structures, thermal properties, names and abbreviations of the diepoxides and diamines used in this study are summarised in Tables 2 and 3.

Diepoxy monomers
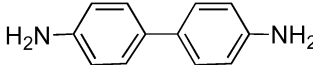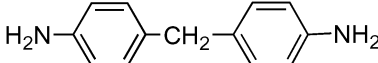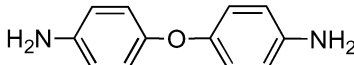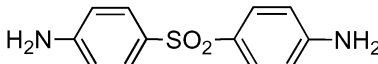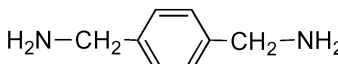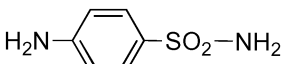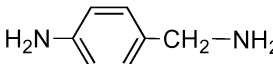
1,4-Phenylenebis(4-(2-(2,3-epoxypropoxy)ethoxy)benzoate) (PEEB) was synthesised as reported by Jahromi *et al.* (*30*) and methyl-1,4-phenylenebis(4-(2, 3-epoxypropoxy)benzoate) (MPEPB) as reported by Mormann and Bröcher (*28*). The diepoxy monomers were further purified by column chromatography (SiO$_2$, CH$_2$Cl$_2$/AcOEt, v/v=85/15).

Preparation of epoxy–amine thermoset samples

A similar procedure was used for each diepoxy–diamine thermoset preparation. A typical example is as follows. Stoichiometric amounts of PEEB (1 g, 1.81 mmol) and benzidine (0.16 g, 0.9 mmol) were dissolved in chloroform (a common solvent) and dried under vacuum at room temperature, to obtain a homogeneous powder. Two NMR tubes (5 mm diameter), previously coated with an anti-adhesive agent (Frekote®), were filled with this powder (sample height 4 cm). One of the tubes was placed at 120–180°C in the high temperature probe (Bruker BVT 3900) of a 250 MHz (5.9 T) NMR spectrometer (Bruker ARX 250) or at 120°C in the probe of a 400 MHz (9.4 T) NMR spectrometer (Bruker MSL 400) previously heated to the reaction temperature. The second tube was cured in the same temperature conditions without any field, inside an oven, for comparison purposes. For the study of reaction kinetics a series of tubes were prepared, cured for various reaction times in the spectrometer and then investigated at room temperature by X-ray scattering.

Table 3. Structures, names, abbreviations and melting temperatures (T_m) of the diamines used in this study.

Type	Diamine (abbreviation)	Structure	T_m /°C
Aromatic symmetric	1,4-diaminobenzene (PDA)	H_2N—⟨benzene⟩—NH_2	143
	4,4′-diaminobiphenyl (benzidine)	H_2N—⟨biphenyl⟩—NH_2	128
	4,4′-methylenedianiline (MDA)	H_2N—⟨⟩—CH_2—⟨⟩—NH_2	90
	4,4′-oxydianiline (APE)	H_2N—⟨⟩—O—⟨⟩—NH_2	191
	bis(4-aminophenylsulfone) (AMS)	H_2N—⟨⟩—SO_2—⟨⟩—NH_2	175
	1,4-di(aminomethyl)benzene (DAPX)	H_2N—CH_2—⟨⟩—CH_2—NH_2	61
Aromatic asymmetric	4-aminobenzenesulfonamide (SAA)	H_2N—⟨⟩—SO_2—NH_2	166
	4-aminobenzylamine (ABA)	H_2N—⟨⟩—CH_2—NH_2	37
Aliphatic	1,4-diaminobutane (DA4)	H_2N–$(CH_2)_4$–NH_2	27
	1,6-diaminohexane (DA6)	H_2N–$(CH_2)_6$–NH_2	43
	1,10-diaminodecane (DA10)	H_2N–$(CH_2)_{10}$–NH_2	62

Analytical techniques

The chemical structure of monomers were confirmed by ^{1}H and ^{13}C NMR (Bruker DRX 500) in CDCl$_3$ using the residual solvent signal as internal reference.

The liquid-crystalline behaviour of epoxy monomers and mixtures was investigated using differential scanning calorimetry (DSC, TA Instruments 2920-modulated DSC equipped with a LNCA TA Instruments cooling device) and polarising optical microscopy (POM, Leitz Laborlux 12 Pol microscope equipped with a Linkam THM 600 heating stage). For both methods, the samples were heated or cooled at a rate of $20°C\,min^{-1}$.

X-ray scattering experiments were carried out using laboratory equipment comprising a Philips PW1830 fixed-tube generator ($\lambda_{CuK\alpha}=1.541$ Å, 40 kV, 30 mA), a graphite monochromator and an evacuated camera (sample-to-detection distance: 67 mm, imaging plates, typical exposure time: 1 h). A single additional experiment was carried out at beamline A2 of the Hasylab (Hamburg) synchrotron radiation facility. The wavelength, λ, was set to 1.500 Å, the sample-to-detection distance was 1.00 m and the detector was a CCD camera. Measurements of linear thermal expansion coefficients (CTE$_{//}$) were performed

on a Netzsch DIL 402 dilatometer, using cylindrical samples (diameter: 5 mm, length: 1 cm).

Determination of the nematic order parameter, S

X-ray scattering is commonly used to determine the mesophase and level of orientation of liquid crystalline materials (*31*). The scattering patterns of nematic (N) materials only exhibit a typical wide-angle diffuse ring at high scattering vector q values ($q=(4\pi\sin\theta)/\lambda$ where 2θ is the scattering angle). The position of this ring in reciprocal space corresponds to the average lateral distance between two mesogens, which typically takes values around $d_1=4$–5 Å. In the case of oriented samples, the alignment degree along the orientation axis (director **n**) can be quantified by the nematic order parameter, S, given by (*32, 33*):

$$S = \frac{1}{2}\left(3\langle\cos^2\beta\rangle - 1\right), \qquad (1)$$

where β is the angle between a particular mesogenic group and the director. S takes values between 0 (isotropic state) and 1 (perfectly oriented state) and can be estimated from the scattering patterns. Qualitatively speaking, S is larger when the wide-angle diffuse
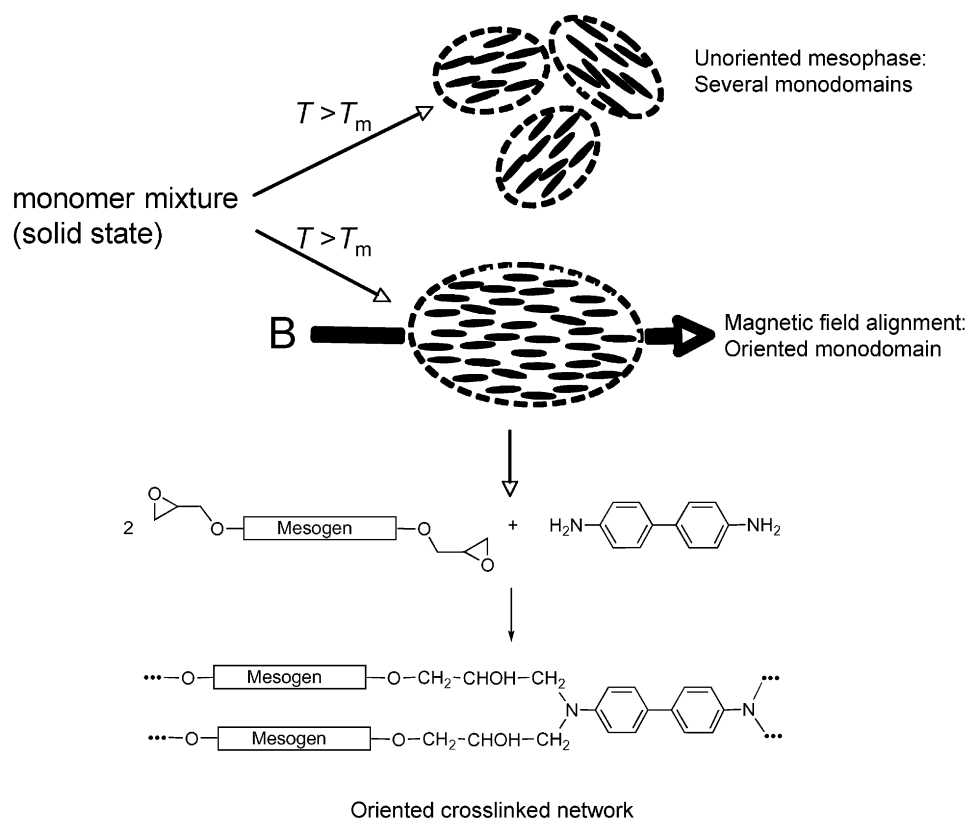

Figure 1. Schematic representation of a diepoxy/benzidine network formation with and without magnetic field alignment.

nematic ring is concentrated around the equator (perpendicular to the director) (*34, 35*). In addition, the scattering pattern of a smectic A (SmA) phase displays diffraction spots (or a diffraction ring if the sample is not oriented) at low *q* values along the meridian, the positions of which give the lamellar period d_2. In this type of mesophase, the mesogens are not only aligned along **n** as in the nematic phase, but also form layers perpendicular to the director (*36*).

3.   Results and discussion

A schematic representation of network formation by the crosslinking reaction between a diepoxide mono-mer and a diamine is shown in Figure 1.

Primary amines react first with epoxies to form secondary amines, which then react with a second epoxy group to form a tertiary amine, creating a crosslink. Upon heating, in the absence of field, a mesophase consists of many small liquid-crystalline domains, each having a specific orientation direction. This organisation is frozen as the system undergoes polymerisation and an unoriented network is obtained (i.e. with no macroscopic orientation). In contrast, when a magnetic field is applied upon heating, all mesogens tend to align along the field and a macroscopically oriented sample is obtained. The crosslinking reaction that occurs upon heating in a magnetic field makes the orientation process very complex. Initially, the unreacted liquid monomer mixture has a very low viscosity, allowing fast orientation. However, when the reaction starts, i.e. on melting of the monomer mixture, viscosity increases sharply until large-scale molecular motions are frozen (*13*). Therefore, the time available to align the sample in the magnetic field is actually very short. The time/temperature conditions at which a liquid crystalline phase is formed before the reaction starts were determined by preliminary DSC and POM studies. Just after melting, all diepoxy–diamine mixtures exhibited the typical texture of nematic LCs. The samples were then cured at 120–180°C in the magnetic field of NMR spectrometers (5.9 and 9.4 T). For each sample a blank experiment was carried out in the same conditions but outside the magnetic field in order to compare structures and degrees of orientation.

Influence of field strength

Extremely strong external fields are not required to induce alignment because the viscosity of the liquid monomer mixture is very low. For instance, Benicewicz *et al.* studied the orientation of EPAMS–SAA networks (Table 1) cured for 1 h at 150°C under various field conditions (*16*). The value of *S* increased with field strength up to *S*=0.7 for a 6 T field. When the field strength was further increased (up to 18 T), no significant improvement of material alignment was observed. Nevertheless, we checked that similar network structures and nematic order parameters were obtained using 5.9 T and 9.4 T fields. Stoichiometric amounts of PEEB and benzidine were crosslinked for 4 h at 120°C in both fields and also outside any field. The scattering patterns of the resulting networks are shown in Figure 2 and the data calculated from these patterns are reported in Table 4. The value of *S* after curing in zero field is 0.37. This value is not trivial and has to be compared with nematic order parameters of other systems cured outside of a magnetic field, which are discussed later on. The order parameters of the samples crosslinked under 5.9 T and 9.4 T (0.82 and 0.84, respectively) are both larger than 0.8, meaning that a very high level of orientation was achieved. The difference between the two values lies within experimental error, showing that there is no need for fields larger than about 6 T.
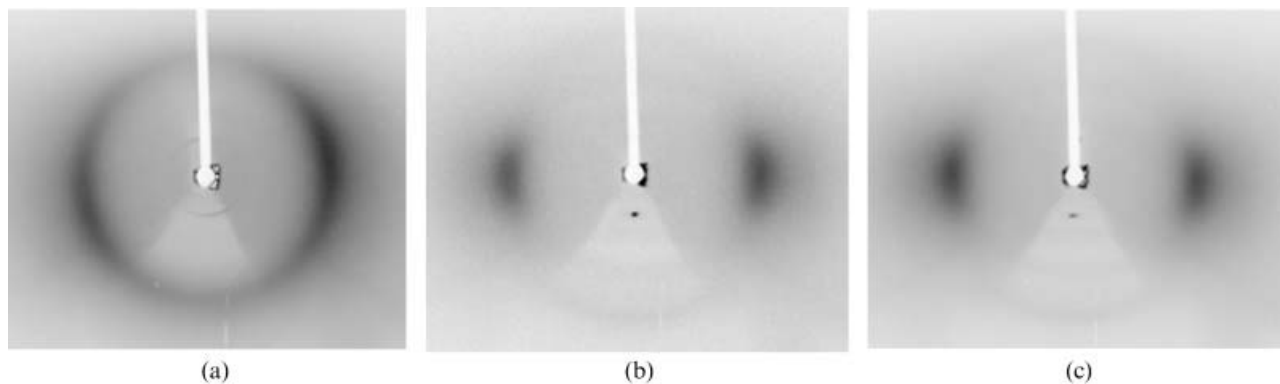

Figure 2. WAXS patterns of PEEB–benzidine networks cured for 4 h at 120°C in various magnetic field conditions: (a) 0 T, (b) 5.9 T and (c) 9.4 T.

Table 4. Nematic order parameter (S), lateral distance between two mesogens (d_1) and lamellar period (d_2) calculated from the WAXS diffraction patterns of PEEB–benzidine networks cured at 120°C for 4 h under various magnetic fields.

Field strength /T	S	d_1 /Å	d_2 /Å
0	0.37	4.3	14.0
5.9	0.82	4.4	12.7
9.4	0.84	4.5	13.3

Table 5. Data calculated from the WAXS patterns of PEEB–benzidine thermosets cured for different times at 120°C in a 5.9 T magnetic field.

Reaction time /min	Mesophase	S	d_1 /Å	d_2 /Å
5	N	0.58	4.3	– [a]
10	N	0.45	4.4	– [a]
15	N	0.62	4.3	– [a]
17	SmA	>0.84	4.3	14.8
30	SmA	0.80	4.3	13.6
45	SmA	>0.84	4.3	12.3
60	SmA	>0.84	4.3	11.8
90	SmA	>0.84	4.3	13.3

[a] The WAXS pattern does not show any small-angle diffraction peak.

Orientation kinetics

The orientation kinetics of the PEEB–benzidine system cured in a 5.9 T field at 120°C, i.e. just above its melting point, was investigated by X-ray scattering (Figure 3 and Table 5).

The scattering patterns exhibit a diffuse ring at large angles, which concentrates around the equator for increasing reaction times, thus reflecting sample orientation. The nematic order parameter reaches S=0.84 at 17 min of reaction time (Figure 3(c)). From 5 to 17 min, a low-intensity diffuse ring is observed at smaller angles (lamellar distance=31 Å). This ring tends to concentrate into a four-spot pattern reminiscent of smectic C fluctuations. This

phenomenon has sometimes been observed with side-chain polymers (37), but has never been reported for LC thermosets. At t=17 min, the order parameter S jumps from 0.6 to more than 0.8 and a SmA diffraction spot appears, meaning that the sample has undergone a N–SmA transition between 15 and 17 min into the reaction (Figure 3(c)). No further changes were observed on the diffraction patterns after this mesophase transition. The same N–SmA transition was observed by Jahromi on this system
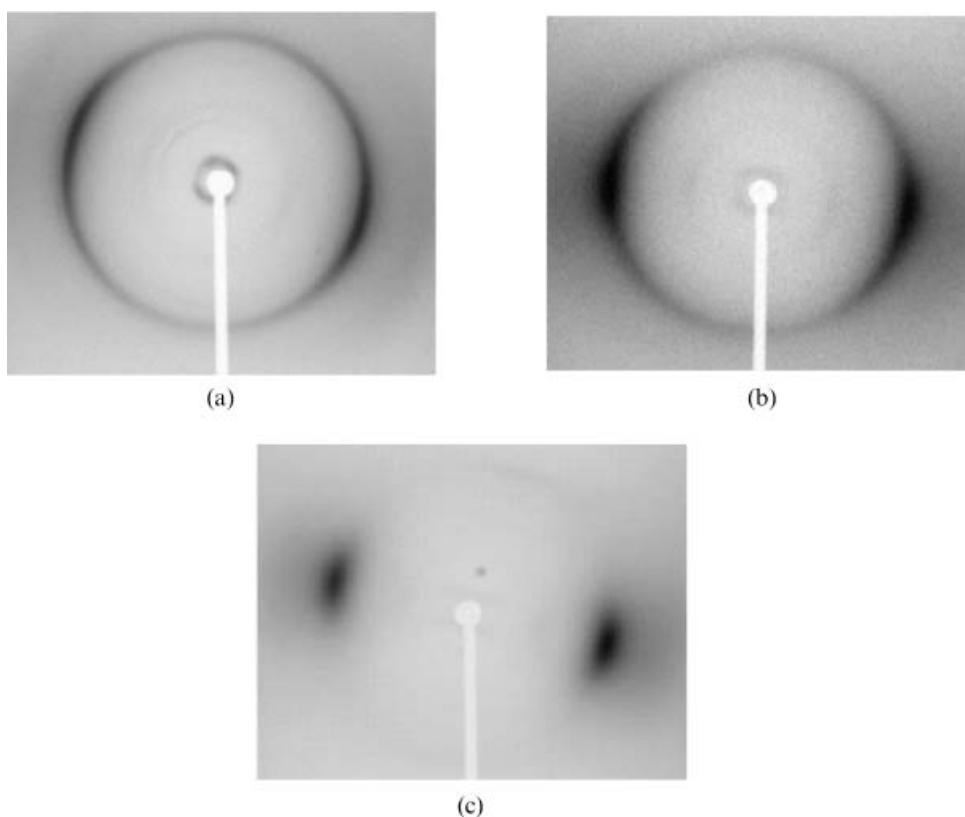

(a)

(b)

(c)

Figure 3. WAXS patterns of PEEB–benzidine networks cured at 120°C in a 5.9 T magnetic field for (a) 5 min, (b) 15 min and (c) 17 min.

after 13 min of curing at 120°C, using ^{2}H NMR spectroscopy and deuterated monomers (*26*).

The results from the WAXS investigation of the MPEPB–benzidine mixture orientation kinetics at 130°C (i.e. just above the melting temperature of this mixture), under a 5.9 T magnetic field, are shown in Figure 4.

Unfortunately, no samples of MPEPB–benzidine network could be obtained before 15 min reaction, since the material was too soft and could not be properly recovered from the NMR tube. The scattering patterns of the samples cured between 15 and 90 min are typical of a SmA mesophase and the nematic order parameter is close to 0.77 for all samples (d_1=4.4–4.5 Å and d_2=11.1–11.5 Å). The maximum level of order of the material is thus reached within the first 15 min of curing at 130°C, during which the N–SmA transition takes place.

Comparison of PEEB– and MPEPB–benzidine thermosets

Figure 5 shows the scattering patterns of both PEEB–benzidine and MPEPB–benzidine thermosets, cured for 10 min at 80°C, then for 30 min at 120°C and finally for 60 min at 160°C (in the case of PEEB networks) or 180°C (in the case of MPEPB networks) under different magnetic field conditions.

The use of several heating steps allowed curing of all samples under similar conditions, compensating for variations in melt temperatures of the monomer mixtures. Furthermore, a curing step at low temperature (close to mixture melting temperature) allows the mesogens to orient in the liquid phase before the gel point is reached. As observed with the unoriented PEEB–benzidine thermoset, the wide-angle diffuse ring of the scattering pattern of the MPEPB–benzidine thermoset cured at zero-field conditions is not very

uniform (Figure 5(a)). However, the degree of orientation was too low to allow a reliable determination of *S*. After curing in a 5.9 T magnetic field (Figure 5(b)), a value of *S*=0.70 was obtained. This is lower than the value of the corresponding PEEB–benzidine thermoset (*S*=0.79) but still corresponds to a fairly high degree of orientation. The diffraction patterns of these two thermosets (Figures 5(b) and 5(c)) are very similar, although they slightly differ at small diffraction angles: the SmA Bragg spot appears more concentrated along the meridian axis on the pattern of the PEEB network, reflecting the better orientation of this sample and also a higher smectic order for this network.

Other PEEB– and MPEPB–diamine thermosets

PEEB– and MPEPB–benzidine networks are highly oriented when cured in a magnetic field. Nevertheless, the structure of the crosslinker (the diamine) could also play an important role in the polymerisation and orientation of the mesogens. Therefore we also synthesised PEEB and MPEPB networks crosslinked with several different diamines. The diamines used were aliphatic, aromatic symmetric or aromatic asymmetric (Table 3). By varying the structure of the diamine we expected to better understand the influence of its structure on the orientation of the final thermoset. Table 6 summarises the data obtained from the WAXS patterns of different diepoxy–diamine thermosets, crosslinked under a 5.9 T magnetic field.

Samples cured in the same conditions but without any field were investigated for comparison and yielded in most cases materials with *S* values in the 0–0.2 range. However, it is noteworthy that relatively high order parameters were measured for the PEEB–benzidine (*S*=0.37) and PEEB–ABA (*S*=0.5) networks. We assume that these high values arise from a
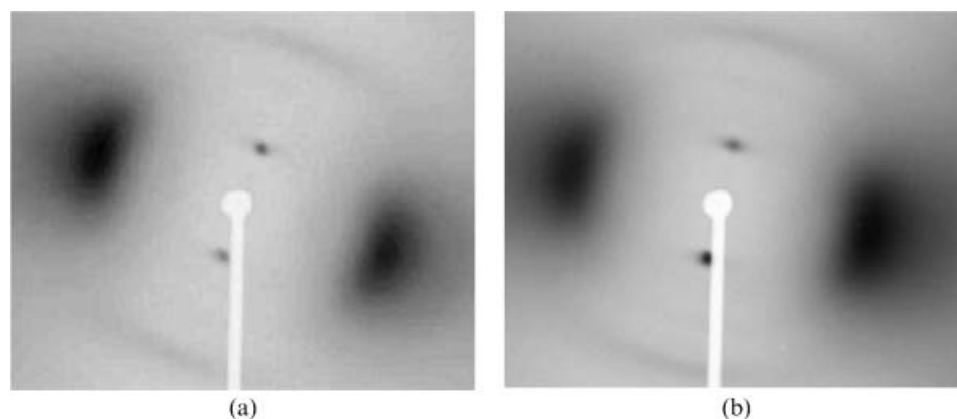

Figure 4. WAXS patterns of a MPEPB–benzidine network cured at 130°C in a 5.9 T magnetic field (a) for 15 min and (b) 30 min.
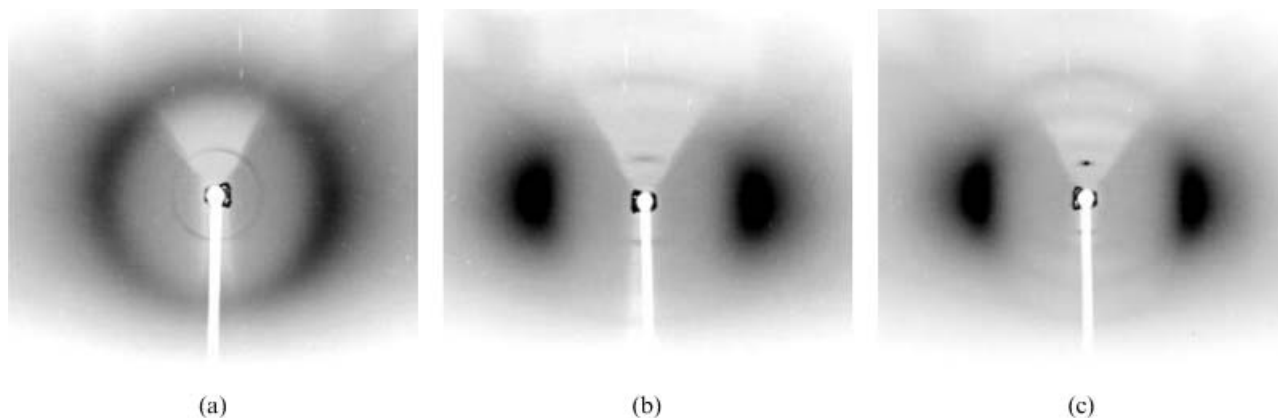
(a)   (b)   (c)

Figure 5. WAXS patterns of PEEB– and MPEPB–benzidine networks cured under various magnetic field conditions 10 min at 80°C, 30 min at 120°C and 60 min at 180°C (in the case of MPEPB networks) or 160°C (in the case of PEEB networks): (a) MPEPB–benzidine, 0 T ; (b) MPEPB–benzidine, 5.9 T; (c) PEEB–benzidine, 5.9 T.

kinetic effect. Indeed, the kinetic study of the PEEB–benzidine network suggests that the mixture mostly contains unreacted monomer during the first minutes of heating. Therefore, the melted monomers can undergo shearing while gently flowing along the tube walls, which aligns the phase and gives rise to the high S value of the resulting network. DSC and POM observations of PEEB–ABA mixtures confirmed that the samples stayed in a liquid state long enough to also undergo shearing alignment. On the contrary, when the crosslinking reaction is fast, as it is the case for MPEPB–benzidine and –ABA mixtures, it prevents any flow and the resulting nematic order parameters are close to 0.

As can be seen in Table 6, not all monomer mixtures cured in the magnetic field led to highly oriented samples. For instance, the S values of thermosets obtained from aliphatic diamines DA4 and DA6 and from aromatic diamines DAPX, APE and AMS were all <0.15 except for the MPEPB–APE

network (S=0.44). The WAXS patterns of some of these samples are shown in Figure 6.

The low degree of orientation obtained with aliphatic diamines and DAPX could be explained by their high basicity and nucleophilicity, inducing a very fast crosslinking reaction that could impede the orientation of the mesogens in the magnetic field. On the contrary, the diepoxy thermosets cured with the less reactive PDA, MDA and asymmetric diamines SAA and ABA exhibit a high level of orientation (Figure 7). It is much more surprising that diepoxy–APE and –AMS thermosets exhibit low S values, as the basicity of these amines is lowered by conjugation with the aromatic ring. These results emphasise the strong influence of the reaction kinetic and of the precursor structures upon the resulting material orientation. For this reason we systematically investigated reaction kinetics as compared to the resulting material orientation on a wide range of epoxy amine networks, using DSC and POM. Detailed results of

Table 6. Mesophase type, nematic order parameter, S, and lamellar distance d calculated from WAXS patterns of various diepoxy–diamine networks cured under a 5.9 T magnetic field 10 min at 80°C, 30 min at 120°C and 60 min at 160°C (for PEEB networks) or 180°C (MPEPB networks).

Diepoxy: Diamine	PEEB			MPEPB		
	Mesophase	S	d_2 /Å	Mesophase	S	d_2 /Å
benzidine	SmA	0.79	13.3	SmA	0.70	11.3
PDA	N	0.54	[a]	SmA	0.70	12.8
MDA	N	0.65	[a]	SmA	0.72	10.8
APE	N	<0.15	[a]	N	0.44	[a]
SAA	N	0.60	[a]	N	0.65	[a]
ABA	N	0.55	[a]	N	0.49	[a]
AMS	N	<0.15	[a]	N	<0.15	[a]
DAPX	N	<0.15	[a]	N	0.20	[a]
DA4	[b]	[b]	[b]	N	<0.15	[a]
DA6	N	<0.15	[a]	N	<0.15	[a]

[a]The WAXS pattern does not show any inner Bragg diffraction peak. [b]Not investigated.
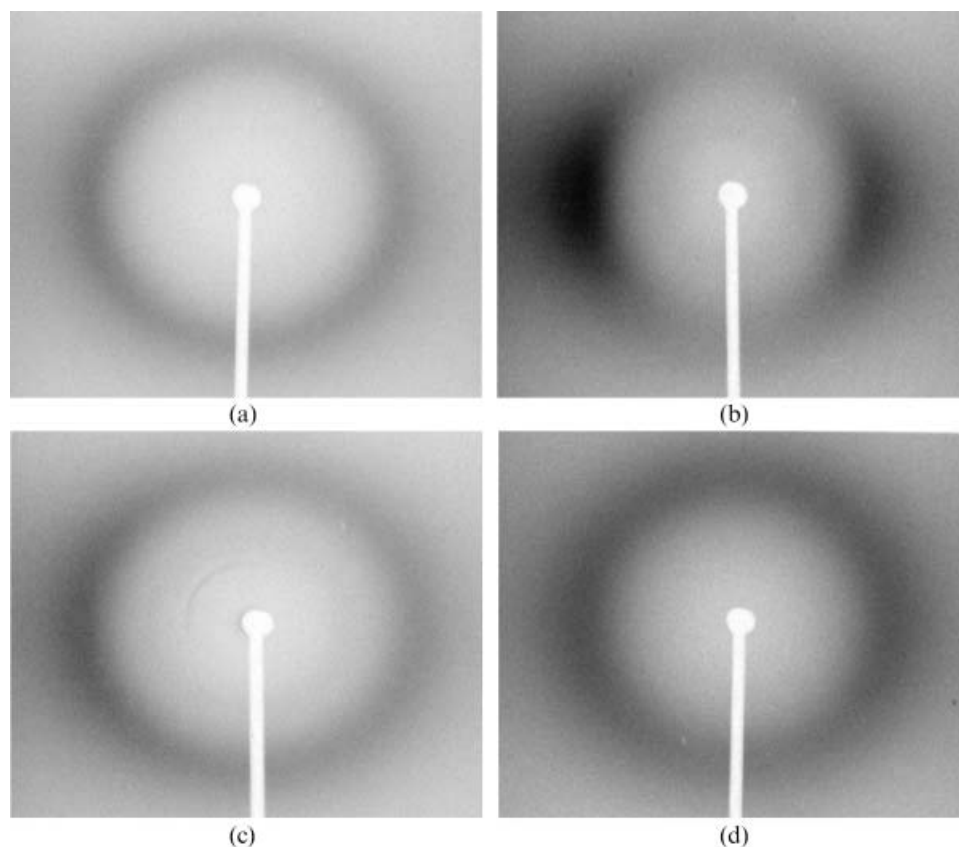
Figure 6. WAXS patterns of various PEEB– and MPEPB–diamine networks cured under a 5.9 T magnetic field 10 min at 80°C plus 30 min at 120°C and 60 min at 160°C (in the case of PEEB networks) or 180°C (in the case of MPEPB networks): (a) PEEB–DAPX; (b) MPEPB–APE; (c) PEEB–AMS; (d) MPEPB–DA6.

this study will be the focus of a forthcoming publication. All thermosets synthesised from SAA and ABA are nematic (Figures 7(c) and 7(d)), although other authors reported that asymmetric diamines favour smectic phase formation (*16*).

In contrast, the PEEB–benzidine, MPEPB–benzidine, MPEPB–PDA and MPEPB–MDA thermosets exhibit SmA phases. As an example, the WAXS pattern of the MPEPB–MDA thermoset is shown in Figure 7e. In principle, the smectic period d_2 corresponds to the repeat distance along the normal axis to the layers. It is not possible, a priori, to determine where the diamine is located in the network and the value of the repeat distance could range anywhere from the length of the diepoxy monomer (e.g. PEEB: 31.5 Å) to the fully extended length of an epoxy monomer bonded to a diamine unit (e.g. PEEB bonded to benzidine: 37 Å). The periods obtained from the scattering patterns of the smectic thermosets lie around 11–13 Å (Table 6). An additional scattering experiment was carried out on the PEEB–benzidine sample using a high flux synchrotron radiation source. It failed to evidence any other

diffraction peak, thus confirming that the smectic period is about 13 Å in this material. These results agree with those reported on unoriented PEEB–benzidine thermosets, where a spacing of 14.1 Å was determined (*38*). On the other hand, some other epoxy–amine networks exhibit spacings close to the length of the polymer repeating unit or only a few angstroms shorter (*39*). In the latter case, the thermosets were frozen in a smectic C phase and thus the difference was simply due to the tilt angle. In our case, the smectic peaks clearly appear along the meridian, and the phase is SmA. The very short spacing observed here is close to the length of benzidine (10 Å) or to the length of the rigid aromatic part of the diepoxy monomer (15 Å). It seems, however, rather awkward to exclude the flexible part of the monomer from the lamellar structure. More complex structures, for instance with interdigitation of mesogens, might be involved in the scattering patterns observed in these networks. Obviously, describing the molecular organisation of these smectic networks in more detail, on the basis of a single Bragg reflection, would be highly questionable.
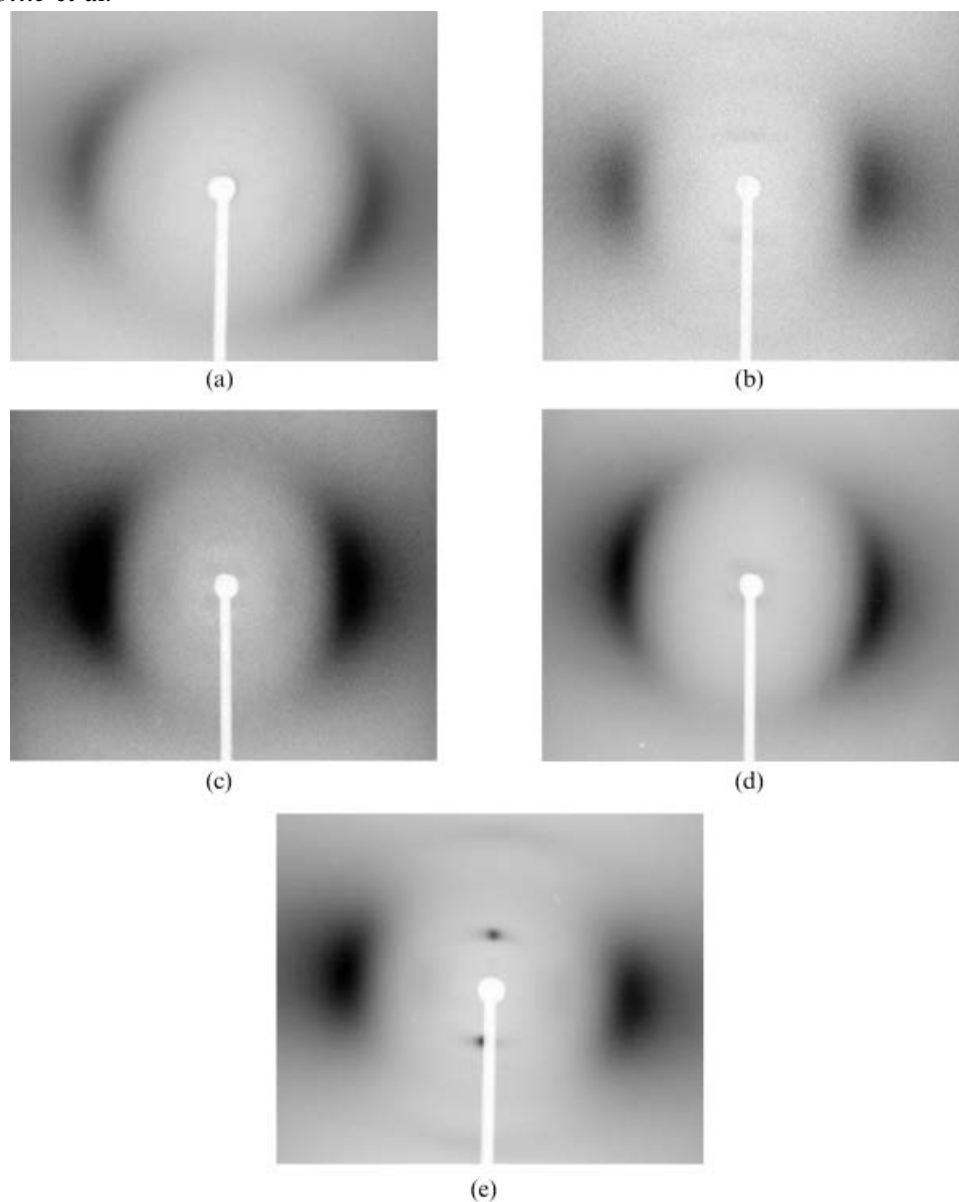
Figure 7. WAXS patterns of various PEEB– and MPEPB–diamine networks cured under a 5.9 T magnetic field 10 min at 80°C plus 30 min at 120°C and 60 min at 160°C (in the case of PEEB networks) or 180°C (in the case of MPEPB networks): (a) PEEB–PDA; (b) MPEPB–PDA; (c) PEEB–SAA; (d) PEEB–ABA; (e) MPEPB–MDA.

Coefficient of thermal expansion (CTE)

Among the specific properties of anisotropic oriented materials, the thermal expansion coefficient along the orientation axis ($CTE_{//}$) is of particular interest. Figure 8 shows the longitudinal thermal expansion of PEEB–benzidine samples cured for 4 h at 120°C in a 9.4 T field and at zero field. At a given temperature, the $CTE_{//}$ value is the slope of the curve.

The thermal behaviours of the two materials differ significantly. The sample cured at zero field presents a weakly positive linear expansion upon heating at temperatures up to 100°C. The slope changes around the glass transition temperature (T_g)

of the network (ca. 117°C) and becomes negative at higher temperatures. In contrast, the linear thermal expansion of the oriented sample is negative within the whole temperature range examined and its absolute value increases sharply above T_g (Table 7). Jahromi et al. obtained similar results with PEEB–benzidine thermosets synthesised under a 9.4 T magnetic field (17). However, below T_g, the absolute value of $CTE_{//}$ reported was about six times lower than the value reported here (-2.6×10^{-6} vs. $-1.50 \times 10^{-5} \, K^{-1}$) (Table 7). The reasons for this discrepancy are not clearly understood, but could be partly due to sample geometry and measurement conditions, which are different in the two studies.
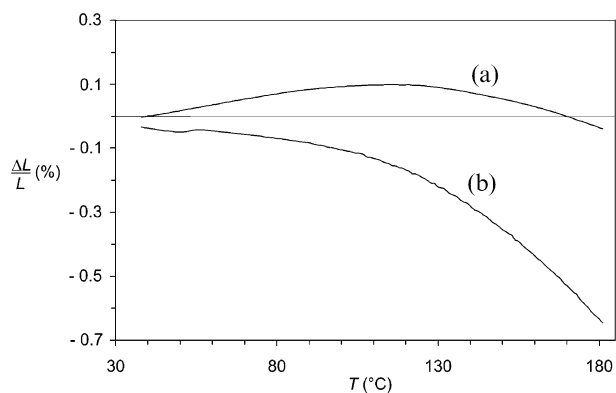
Figure 8. Longitudinal thermal expansion of a PEEB–benzidine network cured 4 h at 120°C (a) under no magnetic field and (b) under a 9.4 T magnetic field.

Table 7. Coefficient of linear thermal expansion along the orientation axis (CTE$_{//}$) for various diepoxy–diamine networks cured in a 5.9 T magnetic field or without any field 10 min at 80°C, 30 min at 120°C and 60 min at 160°C (for PEEB–PDA) or 180°C (for MPEPB networks).

Sample	T_g /°C	CTE$_{//}$ /K^{-1}	
		0 T	5.9 T
PEEB–benzidine[a]	117	1.54×10^{-5} [b]	-1.50×10^{-5} [b,d]
		2.54×10^{-5} [c]	-8.24×10^{-5} [c,d]
PEEB–PDA	99	–	-0.76×10^{-5} [e]
			-4.26×10^{-5} [f]
MPEPB–benzidine	[g]	2.40×10^{-5} [b]	-1.23×10^{-5} [b]
MPEPB–MDA	[g]	–	-2.64×10^{-5} [b]

[a]One-step curing: 4 h at 120°C. [b]Calculated between 40 and 100°C. [c]Calculated between 130 and 180°C. [d]Cured in a 9.4 T field. [e]Calculated between 60 and 80°C. [f]Calculated between 80 and 100°C. [g]No transition detected between 20 and 180°C.

Figure 9 shows the longitudinal thermal expansion curves of various diepoxy–diamine thermosets up to 100°C (i.e. below T_g). Thermosets synthesised outside any magnetic field exhibit a positive linear thermal expansion, as would be expected from their low degree of orientation ($S<0.15$). On the contrary, materials cured in a magnetic field all have negative longitudinal expansion upon heating. The CTE$_{//}$ value of the PEEB–PDA nematic thermoset is significantly lower than those of the smectic thermosets (PEEB–benzidine, MPEPB–benzidine and MPEPB–MDA). This can be understood in view of its lower order parameter, $S=0.54$, versus 0.7 to 0.8 for the smectic ones.

4.   Conclusion

In this work, we investigated the structure and orientation of diepoxy–diamine thermosets obtained by reacting two LC diepoxy monomers (PEEB and MPEPB) with various diamines in a magnetic field. For this purpose, X-ray scattering was extensively used for mesophase identification as well as for determining the nematic order parameter of samples cured under various temperature and magnetic field strength conditions. Very high degrees of orientation along the magnetic field axis were achieved within a
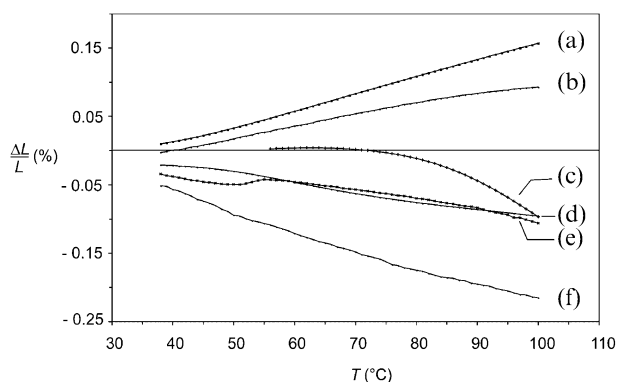

Figure 9. Longitudinal thermal expansion (%) of various PEEB– and MPEPB–diamine networks cured 10 min at 80°C plus 30 min at 120°C and 60 min at 160°C (in the case of PEEB networks) or 180°C (in the case of MPEPB networks): (a) MPEPB–benzidine (0 T); (b) PEEB–benzidine (0 T); (c) PEEB–PDA (5.9 T); (d) MPEPB–benzidine (5.9 T); (e) PEEB–benzidine (9.4 T); (f) MPEPB–MDA (5.9 T).

short reaction time for the diepoxy–benzidine, – MDA, –SAA and–PDA systems. However, not all networks could be oriented. For aliphatic diamines, this phenomenon can be assigned to their high reactivity, which induces a very fast crosslinking reaction that prevents the alignment of the mesogens. All thermosets exhibited nematic or smectic A (SmA) phases. In the case of SmA thermosets, the X-ray scattering patterns were more complicated to interpret than expected. Indeed, the smectic period is smaller than the length of the epoxy monomeric unit, which might be due to a staggered packing of the mesogenic cores. Negative longitudinal thermal expansion coefficients were measured below and above T_g for the materials cured in a magnetic field. These LC epoxy thermosets could, therefore, be interesting alternatives to the ceramics currently used for the thermal compensation of optical devices.

Acknowledgements

References

(1) Ward I.M. *J. Comput. Aided Mater. Des.* **1997**, *4*, 43–52.

(2) de Gennes P.G. In *Polymer Liquid Crystals*; Ciferri A., Krigbaum W.R., Meyer R.B. (Eds), Academic: New York, 1982. pp. 115–131.

(3) Schledjewski R.; Friedrich K. In *Oriented Polymer Materials*; Fakirov S. (Ed.), Huethig & Wepf Verlag: Zug, 1996. pp. 482–506.

(4) Dreher S.; Seifertk S.; Zachmann H.G.; Moszner N.; Mercoli P.; Zanghellini G. *J. Appl. Polym. Sci.* **1998**, *67*, 531–545.

(5) Brostow W.; Jaklewicz M. *J. Mater. Res.* **2004**, *19*, 1038–1042.

(6) Ania F.; Flores A.; Kricheldorf H.R.; Balta-Calleja F.J. *Polymer* **2003**, *44*, 5909–5913.

(7) Brostow W.; Faitelson E.A.; Kamensky M.G.; Korkhov V.P.; Rodin Y.P. *Polymer* **1999**, *40*, 1441–1449.

(8) Anwer A.; Windle A.H. *Polymer* **1993**, *34*, 3347–3357.

(9) Anwer A.; Windle A.H. *Polymer* **1991**, *32*, 103–108.

(10) Shiota A.; Ober C.K. *Macromolecules* **1997**, *30*, 4278–4287.

(11) Kozak A.; Simon G.P.; Williams G. *Polym. Commun.* **1989**, *30*, 102–105.

(12) Shiota A.; Ober C.K. *Prog. Polym. Sci.* **1997**, *22*, 975–1000.

(13) Douglas E.P.; Smith M.E.; Benicewicz B.C.; Earls J.D.; Priester R.D. Jr. In *High Magnetic Fields: Applications, Generation and Materials*; Schneider-Muntau H.J. (Ed.), World Scientific: Singapore, 1997. pp. 31–42.

(14) Barclay G.G.; McNamee S.G.; Ober C.K.; Papathomas K.I.; Wang D.W. *J. Polym. Sci. A* **1992**, *30*, 1845–1853.

(15) Strehmel V. In *Advanced Functional Molecules and Polymers. Vol. 1. Synthesis*; Nalwa H.S. (Ed.), OPA: Amsterdam, 2001. pp. 163–232.

(16) Benicewicz B.C.; Smith M.E.; Earls J.D.; Priester R.D. Jr.; Setz S.M.; Duran R.S.; Douglas E.P. *Macromolecules* **1998**, *31*, 4730–4738.

(17) Jahromi S.; Kuipers W.A.G.; Norder B.; Mijs W.J. *Macromolecules* **1995**, *28*, 2201–2211.

(18) Benicewicz B.C.; Smith M.E.; Earls J.D.; Priester R.D. Jr.; Douglas E.P. *ChemTech* **1997**, *27*, 44–48.

(19) Lincoln D.M.; Douglas E.P. *Polym. Engng Sci.* **1999**, *39*, 1903–1912.

(20) Smith M.E.; Benicewicz B.C.; Douglas E.P.; Earls J.D.; Priester R.D. Jr. *Polym. Prepr.* **1996**, *37*, 50–51.

(21) Smith M.E.; Douglas E.P.; Benicewicz B.C.; Earls J.D.; Priester R.D. Jr. *Mater. Res. Soc. Symp. Proc.* **1996**, *425*, 167–172.

(22) Ober C.K.; Barclay G.G. *Mater. Res. Soc. Symp. Proc.* **1991**, *227*, 281–292.

(23) Barclay G.G.; Ober C.K.; Papathomas K.I.; Wang D.W. *J. Polym. Sci. A* **1992**, *30*, 1831–1843.

(24) Tan C.; Sun H.; Fung B.M.; Grady B.P. *Macromolecules* **2000**, *33*, 6249–6254.

(25) Lee J.Y. *Polym. Bull.* **2006**, *57*, 983–988.

(26) Jahromi S. *Macromolecules* **1994**, *27*, 2804–2813.

(27) Harada M.; Ochi M.; Tobita M.; Kimura T.; Ishigaki T.; Shimoyama N.; Aoki H. *J. Polym. Sci. B* **2004**, *42*, 758–765.

(28) Mormann W.; Bröcher M. *Macromol. Chem. Phys.* **1998**, *199*, 853–859.

(29) Mormann W. In *Polymer Networks Group Review Series;* Vol. 1, te Nijenhuis K., Mijs W.J. (Eds), John Wiley & Sons: New York, 1998. pp. 347–359.

(30) Jahromi S.; Lub J.; Mol G.N. *Polymer* **1994**, *35*, 622–629.

(31) de Gennes P.G.; Prost J. *The Physics of Liquid Crystals,* 2nd ed, Oxford University Press: Oxford, 1993.

(32) Barres O.; Friedrich C.; Jasse B.; Noël C. *Makromol. Chem., Macromol. Symp.* **1991**, *52*, 161–174.

(33) Davidson P.; Petermann D.; Levelut A.M. *J. Phys., Paris II* **1995**, *5*, 113–131.

(34) Leadbetter A.J. In *The Molecular Physics of Liquid Crystals*; Luckhurst G.R., Gray G.W. (Eds), Academic Press: London, 1979.

(35) Mitchell G.R.; Davis F.J.; Ashman A. *Polymer* **1987**, *28*, 639–647.

(36) Noël C. In *Polymeric Liquid Crystals*; Blumstein A. (Ed.), Plenum Press: New York, 1985. pp. 21–63.

(37) Davidson P.; Levelut A.M. *Liq. Cryst.* **1992**, *11*, 469–517.

(38) Jahromi S.; Mijs W.J. *Mol. Cryst. Liq. Cryst.* **1994**, *250*, 209–222.

(39) Shiota A.; Ober C.K. *J. Polym. Sci. A* **1996**, *34*, 1291–1303.